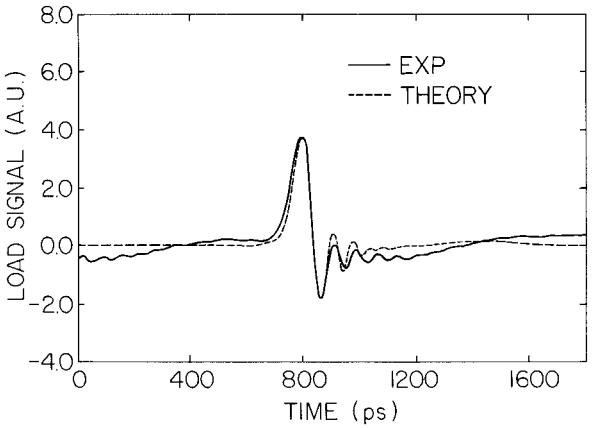

Figure 4 Comparison between theoretical and experimental results of pulse distortion along the CPW/slot-line impedance transformer

simulated results obtained here were satisfactorily supported by practical measurement procedures.

ACKNOWLEDGMENT

The authors acknowledge financial support from TELEBRAS (Brazilian Telecommunications Company) and CNPq (Conselho Nacional de Desenvolvimento Científico e Tecnológico).

REFERENCES

1. C. Hsue and C. Hechtman, Transient responses of an exponential transmission line and its applications to high-speed backdriving in in-circuit test, IEEE Trans Microwave Theory Tech 42 (1994), 458–461.
2. Y. Tang, Z. Li, and S.Y. Tang, Transient analysis of tapered transmission lines used as transformers for short pulses, IEEE Trans Microwave Theory Tech 43 (1995), 1023–1030.
3. T. Itoh, Numerical techniques for microwave and millimeter-wave passive structures, Wiley, New York, 1989.
4. T. Itoh, Spectral domain immitance approach for dispersion characteristics of generalized printed transmission lines, IEEE Trans Microwave Theory Tech MTT-28 (1980), 733–736.
5. R.H. Jansen, Unified user-oriented computation of shielded, covered and open microwave and millimeter-wave transmission line characteristics, Microwave Opt Acoust 3 (1979), 14–22.
6. M.C.R. Carvalho, L.F. Conrado, M. Mosso, and A. Podcameni, Optical analog CATV system conveying 100 channels in a 1.5 GHz subcarrier using the AM-VSB format, Microwave Opt Technol Lett 11 (1996), 215–221.
7. M.C.R. Carvalho, W. Margulis, and J.R. Souza, Microstrip-slot and coplanar waveguide-slot lines with very high dielectric constant substrates for application in high-speed optoelectronics, Microwave Opt Technol Lett 7 (1994), 849–852.

CCC 0895-2477/99

A COAXIAL–RADIAL LINE JUNCTION WITH A TOP LOADING DISK FOR BROADBAND MATCHINGS

Zhongxiang Shen,[1] John L. Volakis,[1] and Robert H. MacPhie[2]
[1] Radiation Laboratory
Department of Electrical Engineering and Computer Science
University of Michigan
Ann Arbor, Michigan 48109-2122
[2] Department of Electrical and Computer Engineering
University of Waterloo
Waterloo, Ont. N2L 3G1, Canada

Received 19 January 1999

ABSTRACT: *A new coaxial–radial transmission-line junction is proposed and characterized by a rigorous full-wave modal-expansion method. The proposed structure modifies the conventional coaxial–radial junction by introducing a circular disk on the top plate of the radial transmission line whose parameters can be adjusted for broadband matchings. Two examples are presented to demonstrate the junction's practicality.* © 1999 John Wiley & Sons, Inc. Microwave Opt Technol Lett 22: 87–90, 1999.

Key words: *waveguide broadband junction; coaxial line; radial line; modal-expansion method*

1. INTRODUCTION

Transitions from a coaxial to a radial line are widely used in microwave and antenna engineering applications. A coaxial–radial junction is often employed in designing power dividers/combiners, coaxial terminations, and antenna feeding structures [1–3]. Previous works on the coaxial–radial junction were experimental or empirical. For example, Allison, Eisenhart, and Greiling [1] developed an equivalent circuit for the coaxial–radial junction, and similar work was carried out by Williamson [2, 4] and Keam and Williamson [5] to characterize coaxial–radial transitions by equivalent circuits. A related problem, that of a cylindrical antenna radiating in a parallel-plate waveguide, was also studied by Otto [7] and Rao [6].

This paper considers a new configuration of the coaxial–radial junction, and describes a rigorous modeling of this structure using the modal-expansion method [8, 9]. The configuration is a modification of the conventional coaxial–radial junction where a circular disk is added on the top plate of the radial line. By changing the parameters of the loading disk, impedance matching can be achieved, and this is demonstrated here. To model the proposed matching structure, the whole junction is divided into several regions, with the fields in each of these expanded in terms of waveguide modes. Subsequently, by enforcing boundary conditions on the structure walls together with field continuity at the region interfaces, we construct a system for determining the modal-expansion coefficients. An optimization algorithm is then employed to minimize the reflection coefficient and to achieve matching at the coaxial–radial junction.

2. FORMULATION

The proposed coaxial-to-radial waveguide transition structure is illustrated in Figure 1. The inner and outer radii of the coaxial line are a_1 and b_1, respectively, and the separation distance between the two plates of the radial waveguide is denoted by d. The dielectric sheath around the inner conductor of the coaxial cable protruding into the radial guide is of

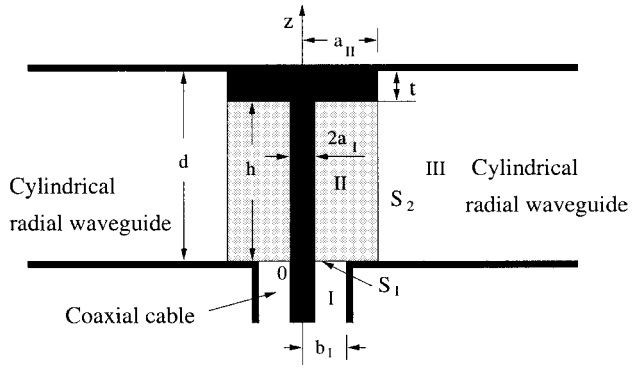

Figure 1 Geometry of a coaxial–radial waveguide transition

permittivity $\epsilon_{r\,\mathrm{II}}\epsilon_0$. The (loading) conducting disk on the top wall of the radial waveguide has a radius a_{II} and a thickness $t = d - h$, as shown.

For analysis, the area around the structure is divided into three regions: I, II, and III. Regions I and III refer to the coaxial line and the radial line, respectively. Region II is the sector occupied by the piece of the coaxial cable protruding into the radial waveguide as defined in Figure 1. Since the structure and the incident mode from the coaxial line are axisymmetric (no ϕ-variation), only three field components (E_z, E_ρ, H_ϕ) are nonzero. Thus, the fields in Region I can be expanded as [8, 9]

$$E_\rho^{\mathrm{I}} = \sum_{n=1}^{N_1} [A_{In}\exp(j\beta_{In}z) + A_{Rn}\exp(-j\beta_{In}z)]e_{In\rho}(\rho) \tag{1a}$$

$$H_\phi^{\mathrm{I}} = \sum_{n=1}^{N_1} [A_{In}\exp(j\beta_{In}z) - A_{Rn}\exp(-j\beta_{In}z)]Y_{In}e_{In\rho}(\rho) \tag{1b}$$

where $\mathbf{A}_I = (A_{I1}, A_{I2}, \ldots, A_{IN_1})^T$ and $\mathbf{A}_R = (A_{R1}, A_{R2}, \ldots, A_{RN_1})^T$ are columns containing the coefficients of the incident and reflected field expansions in coaxial line I. Also, $\beta_{In} = \sqrt{k_0^2\epsilon_{rI} - (x_{In}/a_I)^2}$, with (x_{In}/a_I) being the cutoff wavenumber, defines the propagation constant of the nth mode and Y_{In} denotes the modal admittance. The expression for the normalized transverse modal electric field $e_{In\rho}(\rho)$ is given in [10].

For the air-filled region III (cylindrical waveguide), an appropriate expansion is

$$E_z^{\mathrm{III}} = \sum_{n=0}^{N_3} \frac{A_{3n}}{j\omega\epsilon_0}\cos\frac{n\pi z}{d}\frac{H_0^{(2)}(\gamma_{3n}\rho)}{H_0^{(2)}(\gamma_{3n}a_{\mathrm{II}})} \tag{2a}$$

$$E_\rho^{\mathrm{III}} = \sum_{n=0}^{N_3} \frac{n\pi A_{3n}}{j\omega\epsilon_0 d}\sin\frac{n\pi z}{d}\frac{H_1^{(2)}(\gamma_{3n}\rho)}{\gamma_{3n}H_0^{(2)}(\gamma_{3n}a_{\mathrm{II}})} \tag{2b}$$

$$H_\phi^{\mathrm{III}} = \sum_{n=0}^{N_3} A_{3n}\cos\frac{n\pi z}{d}\frac{H_1^{(2)}(\gamma_{3n}\rho)}{\gamma_{3n}H_0^{(2)}(\gamma_{3n}a_{\mathrm{II}})} \tag{2c}$$

where $(\gamma_{3n})^2 = k_0^2 - (n\pi/d)^2$ and $H_n^{(2)}$ refers to the nth-order Hankel functions of the second kind. As before, $\mathbf{A}_3 = (A_{31}, A_{32}, \ldots, A_{3N_3})^T$ is the matrix column of the expansion coefficients.

Expressions for the fields in Region II can be obtained by employing the resonator method [11]. Specifically, we adapt an expansion which considers Region II as a combination of two resonant regions:

$$E_z^{\mathrm{II}} = \sum_{n=0}^{N_2} \frac{U_n(\rho)}{j\omega\epsilon_r\epsilon_0}A_{2n}\cos\frac{n\pi z}{h} + \sum_{n=1}^{N_1'} B_{2n}e_{2nz}(\rho)\frac{\cosh[\alpha_n(h-z)]}{\sinh(\alpha_n h)} \tag{3a}$$

$$E_\rho^{\mathrm{II}} = \sum_{n=0}^{N_2} \frac{-n\pi U_n'(\rho)}{j\omega\epsilon_{r\,\mathrm{II}}\epsilon_0 h\gamma_{2n}^2}A_{2n}\sin\frac{n\pi z}{h} + \sum_{n=1}^{N_1'} B_{2n}e_{2n\rho(\rho)}\frac{\sinh[\alpha_n(h-z)]}{\sinh(\alpha_n h)} \tag{3b}$$

$$H_\phi^{\mathrm{II}} = \sum_{n=0}^{N_2} \frac{-U_n'(\rho)}{\gamma_{1n}^2}A_{2n}\cos\frac{n\pi z}{h} + \sum_{n=1}^{N_1'} B_{2n}e_{2n\rho}(\rho)\frac{j\omega\epsilon_{r\,\mathrm{II}}\epsilon_0\cosh[\alpha_n(h-z)]}{\alpha_n\sinh(\alpha_n h)}. \tag{3c}$$

Here, $e_{2nz}(\rho)$ and $e_{2n\rho}(\rho)$ are the longitudinal and transverse electric-field components [10] in a coaxial waveguide whose inner and outer radii are a_{I} and a_{II}, respectively [see (1)]. Also, $\alpha_n = \sqrt{(x_n'/a_{\mathrm{I}})^2 - k_0^2\epsilon_{r\,\mathrm{II}}}$ is the attenuation constant of the nth mode, with (x_n'/a_{I}) being its cutoff wavenumber, $(\gamma_{2n})^2 = k_0^2\epsilon_{r\,\mathrm{II}} - (n\pi/h)^2$, and

$$U_n(\rho) = \frac{J_0(\gamma_{2n}\rho)Y_0(\gamma_{2n}a_{\mathrm{I}}) - Y_0(\gamma_{2n}\rho)J_0(\gamma_{2n}a_{\mathrm{I}})}{J_0(\gamma_{2n}a_{\mathrm{II}})Y_0(\gamma_{2n}a_{\mathrm{I}}) - Y_0(\gamma_{2n}a_{\mathrm{II}})J_0(\gamma_{2n}a_{\mathrm{I}})} \tag{4}$$

with J_0 and Y_0 being the zeroth-order Bessel functions of the first and second kind, respectively.

The coefficients in the above expansions can be readily determined by enforcing tangential field continuity (for both $\vec{E}$ and $\vec{H}$) across the adjacent regions. Continuity between Regions I and II ($a_{\mathrm{I}} < \rho < b_1$, $z = 0$) gives the relation

$$\mathbf{B}_2 = \mathbf{M}_a(\mathbf{A}_I + \mathbf{A}_R) \tag{5}$$

$$\mathbf{Y}_I(\mathbf{A}_I - \mathbf{A}_R) = \mathbf{M}_b\mathbf{A}_2 + \mathbf{M}_a^T\mathbf{D}_2\mathbf{B}_2 \tag{6}$$

where $\mathbf{M}_a$, $\mathbf{D}_2$, and $\mathbf{M}_b$ refer to the mode-matching coupling matrices whose elements are given by

$$M_{an,m} = 2\pi\int_{s_1} e_{2n\rho}(\rho)e_{1m\rho}(\rho)\rho\,d\rho$$

$$D_{2n,m} = \frac{j\omega\epsilon_r\epsilon_0}{\alpha_n\tanh(\alpha_n h)}\delta_{n,m}$$

$$M_{bn,m} = 2\pi\int_{s_1}\frac{-U_m'(\rho)}{\gamma_{2m}^2}e_{1n\rho}(\rho)\rho\,d\rho.$$

Also, $\mathbf{A}_I$, $\mathbf{A}_R$, $\mathbf{A}_2$, and $\mathbf{B}_2$ denote the columns containing the modal-expansion coefficients.

Similarly, on enforcing continuity at S_2 ($0 < z < d$, $\rho = a_{\mathrm{II}}$) and employing mode orthogonality, we get

$$\mathbf{A}_3 = \mathbf{W}\mathbf{A}_2 \tag{7}$$

$$-\mathbf{G}\mathbf{A}_2 + \mathbf{M}_c\mathbf{B}_2 = \mathbf{F}\mathbf{Y}_3\mathbf{A}_3 \tag{8}$$

where the elements of the mode-matching coupling matrices $\mathbf{W}$, $\mathbf{G}$, $\mathbf{M}_c$, $\mathbf{F}$, and $\mathbf{Y}_3$ are given by

$$W_{n,m} = \frac{1}{\epsilon_{r\,\mathrm{II}}} F_{m,n}, F_{n,m} = \int_0^h \cos\frac{m\pi z}{d}\cos\frac{n\pi z}{h}\,dz$$

$$M_{cn,m} = e_{2m\rho}(a_{\mathrm{II}})\int_0^h \frac{j\omega\epsilon_{\mathrm{II}\,r}\epsilon_0\cos[\alpha_m(h-z)]}{\alpha_m \sinh(\alpha_m h)}\cosh\frac{n\pi z}{h}\,dz$$

$$= e_{2m\rho}(a_{\mathrm{II}})\frac{j\omega\epsilon_0\epsilon_{r\,\mathrm{II}}}{(n\pi/h)^2 + \alpha_m^2}$$

$$G_{n,m} = \frac{hU_n'(a_{\mathrm{II}})}{\epsilon_n\gamma_{2n}^2}\delta_{n,m}, Y_{3n,m} = \frac{\epsilon_n H_1^{(2)}(\gamma_{3n}a_{\mathrm{II}})}{d\gamma_{3n}H_0^{(2)}(\gamma_{3n}a_{\mathrm{II}})}\delta_{n,m}$$

with $\epsilon_n = 1$ for $n = 0$, $\epsilon_n = 2$ for $n > 0$, and $\delta_{n,m} = 1$ for $n = m$, $\delta_{n,m} = 0$ for $n \neq m$.

Finally, on combining Eqs. (5)–(8), we readily obtain the matrix system

$$\mathbf{A}_R = \mathbf{S}_{11}\mathbf{A}_I = \left[2(\mathbf{I} + \mathbf{Y}_I^{-1}\mathbf{Y}_L)^{-1} - \mathbf{I}\right]\mathbf{A}_I \tag{9}$$

where

$$\mathbf{Y}_L = \left[\mathbf{M}_b(\mathbf{G} + \mathbf{F}\mathbf{Y}_3\mathbf{W})^{-1}\mathbf{M}_c + \mathbf{M}_a^T\mathbf{D}_2\right]\mathbf{M}_a. \tag{10}$$

These refer to infinite systems, and must be truncated up to a certain number of attenuating modes to obtain a finite invertible system for solution. Note that in (9), $\mathbf{A}_I = (A_{I1}, A_{I2}, \ldots, A_{IN_1})^T$ represents the coefficients of the incident mode within the coaxial line. Also, upon solving for $\mathbf{A}_R$ via (9), we can then proceed to obtain the coefficients in other expansions.

3. NUMERICAL EXAMPLES

As an initial validation of the formulation described in the preceding section, we first consider the case of a cylindrical antenna radiating in a parallel-plate waveguide. For this case, we choose $a_{\mathrm{II}} = b_{\mathrm{I}}$, $d = h$, and $\epsilon_{r\,\mathrm{II}} = 1$, for which numerical results are available in the literature. Computed results for the input admittance of an antenna in a parallel-plate waveguide using our modal-expansion method are given in Figure 2. These data were generated by setting $N_1 = N_1' = 2$ and $N_3 = N_2 = 40$, and are seen to compare very well with results from Otto [7].

Next, we present two example designs of the proposed coaxial–radial waveguide transition. As in [8, 9], $N_1' = [(a_{\mathrm{II}} - a_{\mathrm{I}})/(b_{\mathrm{I}} - a_{\mathrm{I}})]N_1$ and $N_3 = (d/h)N_2$ for the modal expansions to ensure convergent results. The first example design is a transition from a 50 Ω coaxial line (TNC connector) to a radial waveguide at *C*-band. The inner and outer radii of the coaxial line are 1.08 and 3.5 mm, respectively, and the coaxial line is filled with Teflon having $\epsilon_{r\mathrm{I}} = 2.0$. The optimized parameters for the junction were found to be $a_{\mathrm{II}} = 7.5$ mm, $h = 5.35$ mm, and $d = 6.6$ mm with $\epsilon_{r\,\mathrm{II}} = 4.3$ (referring to boron nitride). For these values, the calculated VSWR at the coaxial line port is shown in Figure 3. We observe that the optimized VSWR of this transition is better than 1.16 (return loss of 23.5 dB) over the whole *C*-band (3.4–4.2 GHz).

The second design example is a transition from a 50 Ω coaxial line (SMA) to a radial waveguide at *X*-band. For this case, the optimized parameters of the junction were found to be $a_{\mathrm{II}} = 3.3$ mm, $h = 2.4225$ mm, $d = 2.782$ mm, and $\epsilon_{r\,\mathrm{II}} = 4.3$ with $a_I = 0.635$ mm, $b_{\mathrm{I}} = 2.06$ mm, $\epsilon_{r\mathrm{I}} = 2.0$ for the coaxial line. The VSWR at the coaxial line port calculated by our modal-expansion method is illustrated in Figure 4. As seen, the VSWR of the transition is less than 1.2175 (return loss of better than 20 dB) over the entire *X*-band (8.0–12.0 GHz).

4. CONCLUSION

We have described a new coaxial–radial waveguide junction with additional control parameters for achieving broadband matching. A mode-matching method was proposed and employed for the analysis of this junction. Two design examples were given to illustrate the practicality of the junction.

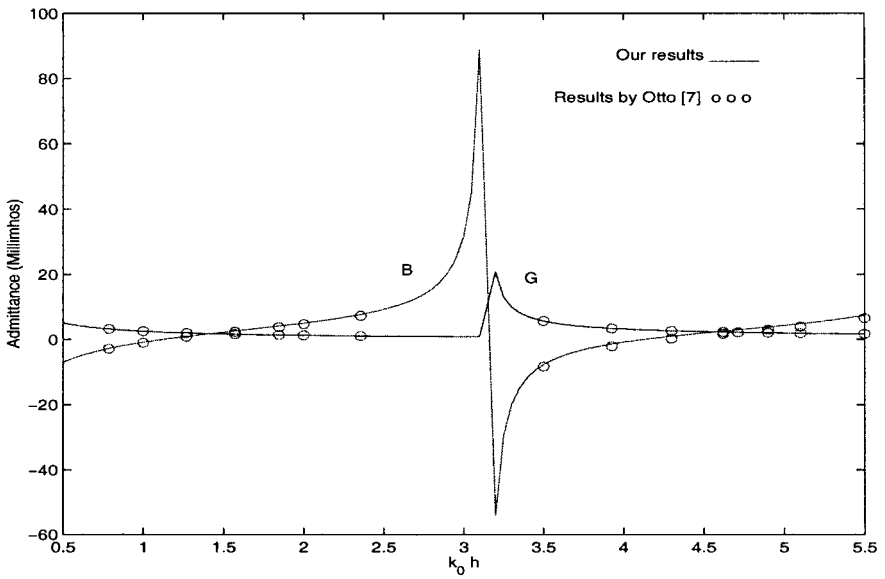

Figure 2 Admittance of a cylindrical antenna in a parallel-waveguide ($ka_{\mathrm{I}} = 0.0664$, $a_{\mathrm{II}} = b_{\mathrm{I}} = 2.25a_{\mathrm{I}}$, $d = h$, $\epsilon_{r\,\mathrm{II}} = 1$)

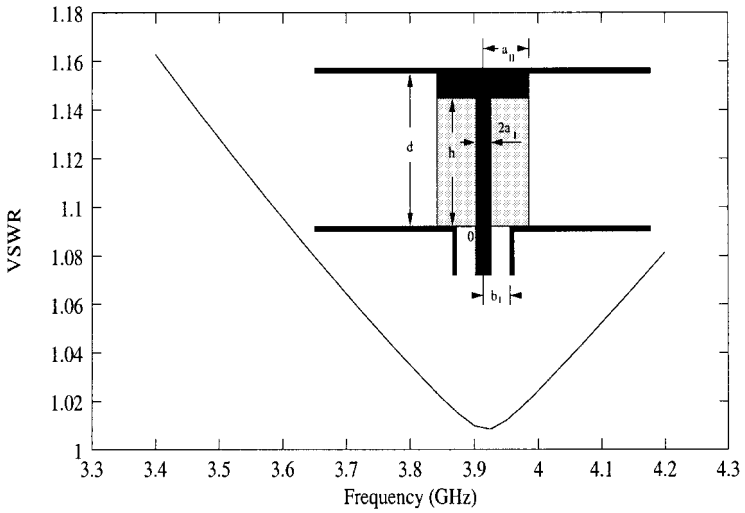

Figure 3 Calculated VSWR of a coaxial–radial waveguide transition at C-band ($a_{\mathrm{II}} = 7.5$ mm, $h = 5.35$ mm, $d = 6.6$ mm, $\epsilon_{r\,\mathrm{II}} = 4.3$)

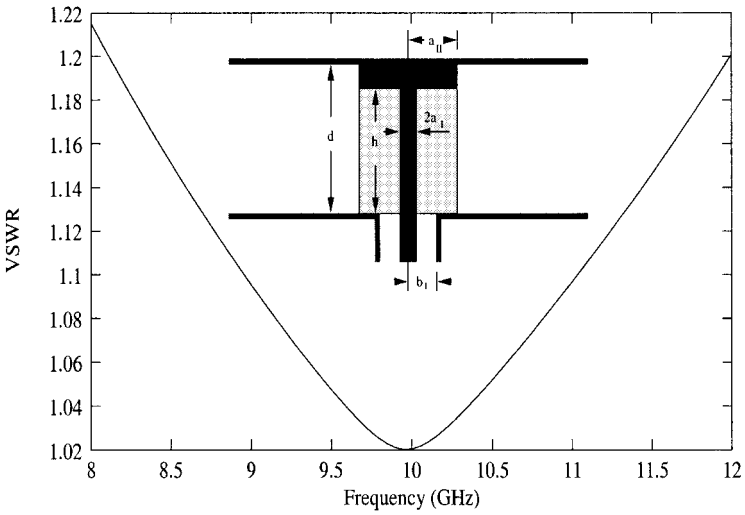

Figure 4 Calculated VSWR of a coaxial–radial waveguide transition at X-band ($a_{\mathrm{II}} = 3.3$ mm, $h = 2.4225$ mm, $d = 2.782$ mm, $\epsilon_{r\,\mathrm{II}} = 4.3$)

ACKNOWLEDGMENT

One of the authors (Z. Shen) would like to acknowledge support from the Natural Sciences and Engineering Research Council (NSERC) of Canada under a Postdoctoral Fellowship.

REFERENCES

1. R.C. Allison, R.L. Eisenhart, and P.T. Greiling, A matched coaxial-radial transmission line junction, IEEE MTT-S Int Microwave Symp Dig, 1978, pp. 44–46.
2. A.G. Williamson, Radial-line/coaxial line junction: Analysis and equivalent circuits, Int J Electron 58 (1985), 91–104.
3. M. Takahashi, J. Takada, M. Ando, and N. Goto, A slot design for uniform aperture field distribution in single-layered radial line slot antennas, IEEE Trans Antennas Propagat 39 (1991), 951–959.
4. A.G. Williamson, Equivalent circuits for radial-line/coaxial-line junction, Electron Lett 17 (1981), 300–301.
5. R.B. Keam and A.G. Williamson, Analysis of a general coaxial-line/radial-line region junction, IEEE Trans Microwave Theory Tech 41 (1991), 516–519.
6. B.R. Rao, Current distribution and impedance of an antenna in a parallel-plate region, Proc Inst Elect Eng 112 (1965), 259–265.
7. D.V. Otto, The admittance of cylindrical antennas driven from a coaxial line, Radio Sci 2 (1967), 1031–1042.
8. Z. Shen and R.H. MacPhie, Rigorous evaluation of the input impedance of a sleeve monopole by modal expansion method, IEEE Trans Antennas Propagat 44 (1996), 1584–1591.
9. Z. Shen and R.H. MacPhie, Modal expansion analysis of monopole antennas driven from a coaxial line, Radio Sci 31 (1996), 1037–1046.
10. N. Marcuvitz, Waveguide handbook, McGraw-Hill, New York, 1951.
11. E. Kuhn, A mode-matching method for solving field problems in waveguide and resonator circuits, AEU 27 (1973), 511–518.

CCC 0895-2477/99